JOURNAL OF MATERIALS SCIENCE **38** (2003) 1243–1248

Preparation and optical properties of gold nanoparticles embedded in barium titanate thin films

YONG YANG, JIANLIN SHI, WEIMING HUANG, SHUGANG DAI, LIN WANG
State key Lab of High Performance Ceramics and Superfine Microstructure, Shanghai Institute of Ceramics, Chinese Academy of Science, 1295 Dingxi Road, Shanghai 200050, People's Republic of China
E-mail: yywfx@hotmail.com

High amount of gold nanoparticles was successfully incorporated into amorphous $BaTiO_3$ thin films by sol-gel process. Thiourea was applied to prevent Au ions from being reduced and aggregating as the effective stabilization agents. These films exhibited unique surface plasma resonance red-shifting and particular changes of surface plasma resonance intensity with the increase of heat-treating temperature, which could be attributed to the influence of $BaTiO_3$ ferroelectric domains. The films also exhibited superfast nonlinear optical response and larger third-order nonlinear susceptibility $\chi^{(3)}$, which was attributed to hot electron contribution.

1. Introduction

Noble metal nanoparticles embedded in a dielectric medium have been reported to exhibit some attractive optical properties, such as high third-order nonlinear susceptibility $\chi^{(3)}$, ultra-fast nonlinear optical response [1–4], surface plasma resonance absorption occurring in the near-uv or visible region [5, 6], which would have potential applications in nonlinear optical devices such as optical computing, real time holography, optical correlators, and phase conjugators [7].

Noble metal nanoparticles incorporated into dielectric matrix such as ZrO_2 [8], SiO_2 [9, 10], and TiO_2 [11] thin films have been prepared and extensively studied. The surface plasma resonance (SPR) phenomenon and the quantum size effect [12] have attracted much interests. Barium titanate thin films have high dielectric constants and high refractive indices, which could strongly influence the local fields around the metal particles [13]. Recently, barium titanate thin films incorporated with noble metal nanoparticles [14, 15] have been investigated, but the amount of metal particles dispersed in these films was very low (Au molar amount $< 10\%$) and the influence of $BaTiO_3$ matrix was not discussed.

In order to obtain a suitable nonlinear optical material which has high $\chi^{(3)}$, a possible strategy might be to incorporate a large amount of metallic particles into the matrix and to control the shape and size of metallic particles [1, 12]. The sol-gel technique could be a suitable method to prepare such nanocomposite materials because this method usually permits us to incorporate a large amount of metal particles into thin films and control the dimensions and shapes of the particles [12]. Many reports have concentrated on the sol-gel preparation of gold nanoparticles embedded into films [8, 15, 16]. In that approach, a solution of Au^{3+} ions (commonly the tetrachloroaurate anion $[AuCl_4]^-$) was generally added into the matrix sol, and gold nanoparticles were obtained thermally by heating the doped film. But there are some problems encountered with this procedure. Firstly, Au^{3+} ions are easily and quickly reduced to Au atoms and rapidly agglomerate when Au^{3+} ions are added into sol. It is very difficult to control this procedure. Furthermore, metallic gold particles are easily precipitated on the film surface and aggregate into big particles, so the particle size distribution is broad. In order to overcome these problems, we applied a new synthesis procedure, which avoids gold precipitation in the sol and on the film surface. The technique is based on the substitution of the chloro ligands of $[AuCl_4]^-$ with thiourea ligands, which can form stable Au-thiourea complexes [16]. In this work, high amount of Au nanoparticles (Au molar amount $= 20\%$) has been successfully incorporated into $BaTiO_3$ thin films, which exhibited high third-order nonlinear susceptibility and the influence of self-polarization on SPR intensity of gold particles.

2. Experimental

$HAuCl_4 \cdot 4H_2O$, $Ba(CH_3COO)_2$ and titanium butoxide were used as starting materials to prepare gold-dispersed barium titanate thin films through a sol-gel process. $BaTiO_3$ precursor solution and $HAuCl_4$-ethanol solution were prepared separately, and mixed together to form composite precursor solution.

To make $BaTiO_3$ precursor solution, $Ba(CH_3COO)_2$ (2.55 g, 10 mmol) was dissolved in an aqueous mixed solution of acetic acid (10 ml) and 2-methoxyethanol (10 ml). After stirring the solution for 30 min at room temperature, appropriate amount of acetylacetone was

added to stabilize the solution. This was followed by an addition of titanium butoxide (3.4 ml) and stirred for another 30 min. Finally, the solution was filtrated with 0.22 um filter paper, then aged for one week. $HAuCl_4$-ethanol solutions were prepared by dissolving $HAuCl_4 \cdot 4H_2O$ (1.0 g) into 2-methoxyethanol (10 ml). $Au/BaTiO_3$ composite precursor solution was prepared by injecting $HAuCl_4$ solutions into $BaTiO_3$ precursor solution slowly with molar ratio of Au/Ba = 1:5 and stirring about 20 min. This composite solution was yellow and clear. But Au^{3+} ions were easily reduced into Au atoms in the acid solution and the composite solution turned opaque after twenty minutes. In order to increase the stability of the corresponding gold sol, the ligands solution of thiourea dissolved in ethanol was introduced into $HAuCl_4$-ethanol solutions with molar ratio of Au/S = 1:5 before being added into $BaTiO_3$ precursor sol. Au-dispersed $BaTiO_3$ thin films were coated on glass or quartz glass slides by dip-coating method at withdrawal speed 25–150 mm/min. Each film was dried at 60°C for 10 min and successively heated to 200–1000°C for 20 min in N_2 atmosphere. The colors of films turned light purplish blue when they were heat-treated.

The crystallographic structure of $Au/BaTiO_3$ films was investigated in Rigaku D/Max RB X-ray diffractometer operated at 50 kv and 140 mA using Cu K_a by grazing-incident small-angle X-ray diffraction method; the grazing angle of the incident beam against the surface of the sample was fixed at 2°. The diffracted X-ray was collected by scanning in 0.1° step and counting 4 seconds. The microstructure of the films was analyzed by transmission electron microscope (JEM 2010 high resolution analytical transmission electron microscope). The absorption spectra were measured by UV-VIS-NIR scanning spectrophotometer (UV-3101 PC, SHIMADZU). The refractive indices were measured by ellipsometry (V-VASE with AutoRetarder, J. A. Woollam). The values of $\chi^{(3)}$ were estimated in accordance with OKE (Optical Kerr effect).

3. Results and discussion

3.1. The phase structure of $Au/BaTiO_3$ films

Fig. 1a shows the X-ray diffraction (XRD) patterns of $Au/BaTiO_3$ thin films coated on glasses, which are heat-treated at different temperatures ranging from 200°C to 600°C. Two peaks at $2\theta = 38.3°$ and 44.5° in those films annealed at 400°C and 600°C can be indexed to Au (111) and Au (200) crystalline planes of the Fcc lattice structure, respectively. But it is not so apparent in these films annealed at 200°C, because the crystalline structure is not integrated. The characteristic diffraction peaks of $BaTiO_3$ matrix can not be found in scanning range, which indicates that the $BaTiO_3$ matrix is amorphous up to 600°C. $BaTiO_3$ crystallite phase can be found in thin films annealed at 800°C as shown in Fig. 1b.

3.2. TEM images

The TEM images of samples annealed at 400°C, which were not treated with thiourea, are shown in Fig. 2a. There are two different kinds of gold nanoparticles:

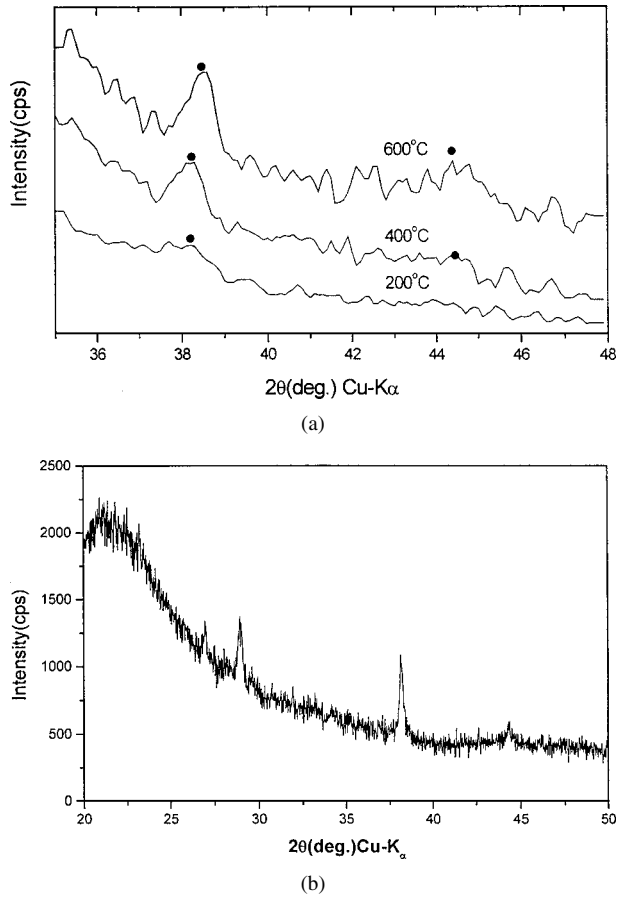

Figure 1 (a) Small-angle XRD patterns of $Au/BaTiO_3$ films coated on glass with different annealing temperature and (b) XRD pattern of $Au/BaTiO_3$ film annealed at 800°C.

small spherical particles with a size of 15 nm and larger particles with a size of 60 nm. It can be interpreted as follows: some Au^{3+} ions had been reduced to Au atoms due to the presence of carboxyl group in the early stage of gel aging and drying, and easily aggregated into larger particles before thermal diffusion could disperse them in the heat-treating process [16]. When Au^{3+} ions were complexed with thiourea, the Au^{3+}-thiourea complexes remained stable during the period of gel aging and drying. Small Au particles could form due to the decomposition of Au^{3+}-thiourea complexes in the high temperature heating process. It is also proved by the TEM images of the sample treated by thiourea as shown in Fig. 3a. There is only one kind of homogeneous spherical gold particles with size of 10 nm. The average crystalline size of Au particles determined from TEM increases with the increase of annealing temperature (not shown). The electron diffraction patterns of gold nanoparticles embedded in $BaTiO_3$ film are shown in Figs 2b and 3b, respectively. Polycrystalline structures of Au particles can be identified from weak rings and some scattered spots clearly.

3.3. Refractive index

The refractive indices of thin films change with annealing temperature as shown in Fig. 4. With the increase of temperature, water and organic gas continually vaporized and the refractive indices of thin films increased. When annealing temperature was higher than 600°C, water and organic gas were totally lost

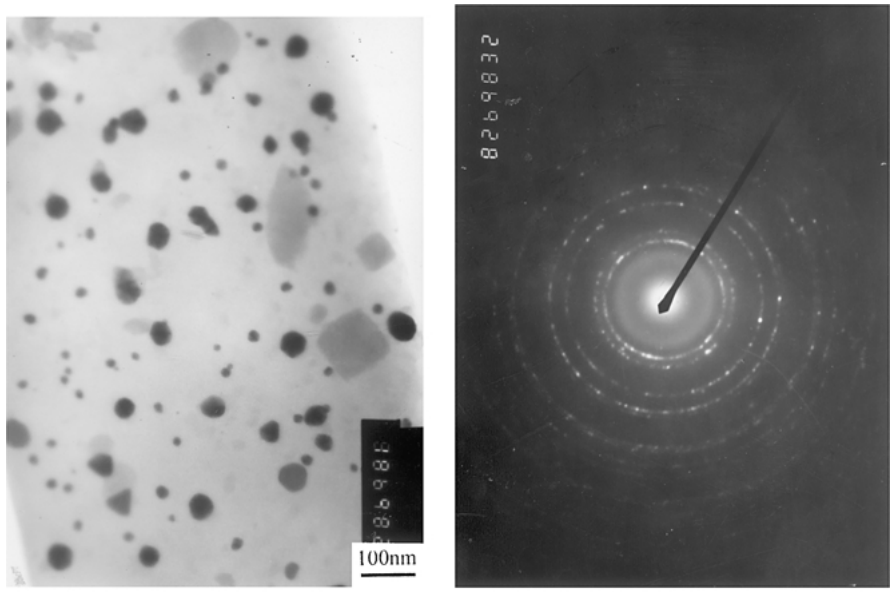

Figure 2 (a) TEM images of Au/$BaTiO_3$ film annealed at 400°C and (b) The electron diffraction pattern of Au particles.

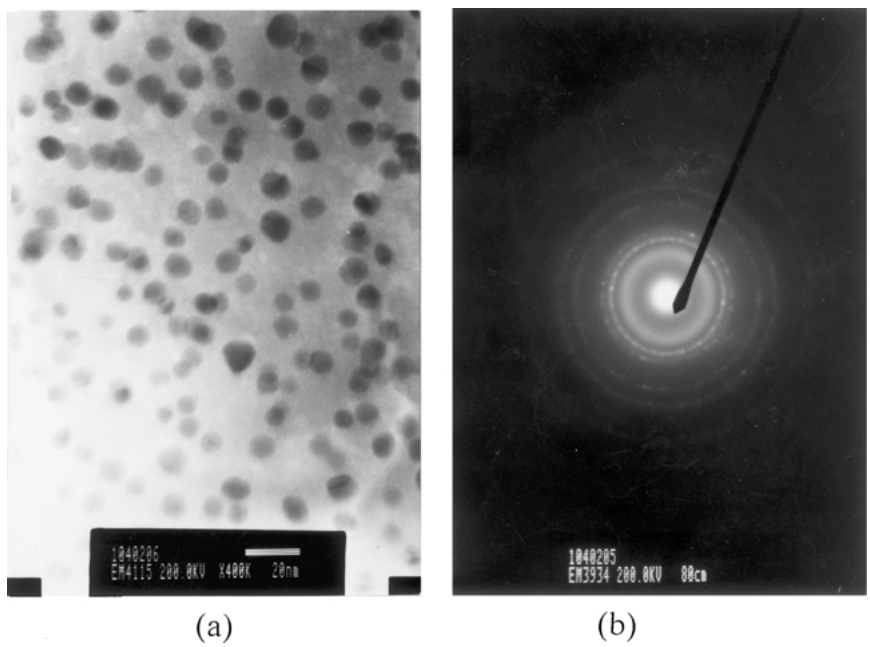

Figure 3 (a) TEM images of Au/$BaTiO_3$ film annealed at 400°C (treated by thiourea) and (b) The election diffraction pattern of Au particles.

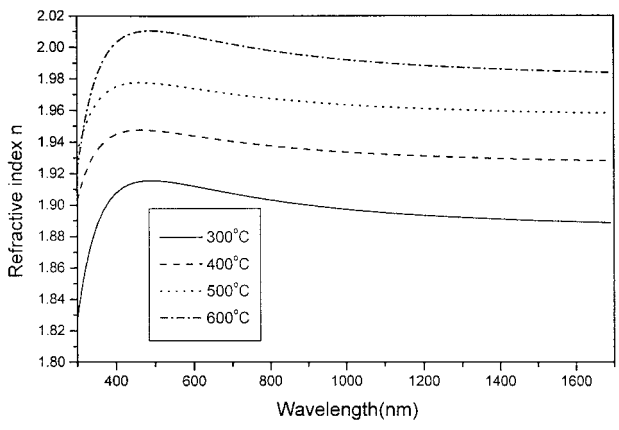

Figure 4 The refractive indices of Au/$BaTiO_3$ films annealed at different temperatures.

and an amorphous-to-crystalline transition took place with subsequent phase transitions, which was accompanied by large porosity reduction. Different structural arrangements could also be obtained with increasing the annealing temperatures, leading to continuous increases of refractive indices of the thin films [15].

3.4. Optical absorption spectra

Fig. 5a shows the changes of the films' absorption spectra at different heat-treatment temperature, which corresponds to different absorption peaks at 569.5 nm (200°C), 579.5 nm (300°C), 583.5 nm (400°C), 595.5 nm (500°C), 605.5 nm (600°C). The absorption peaks, which are attributed to the surface plasma resonance of gold particles [15], shift to longer wavelength

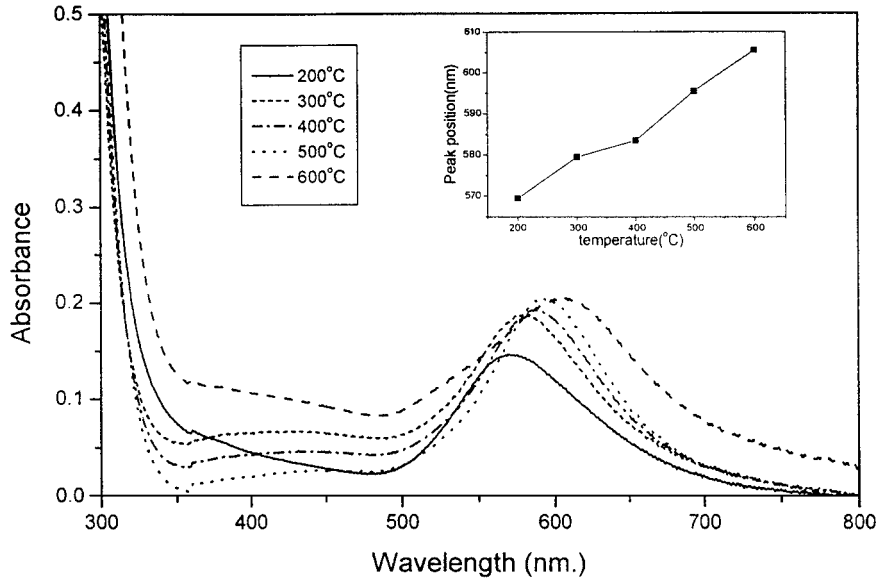

(a)

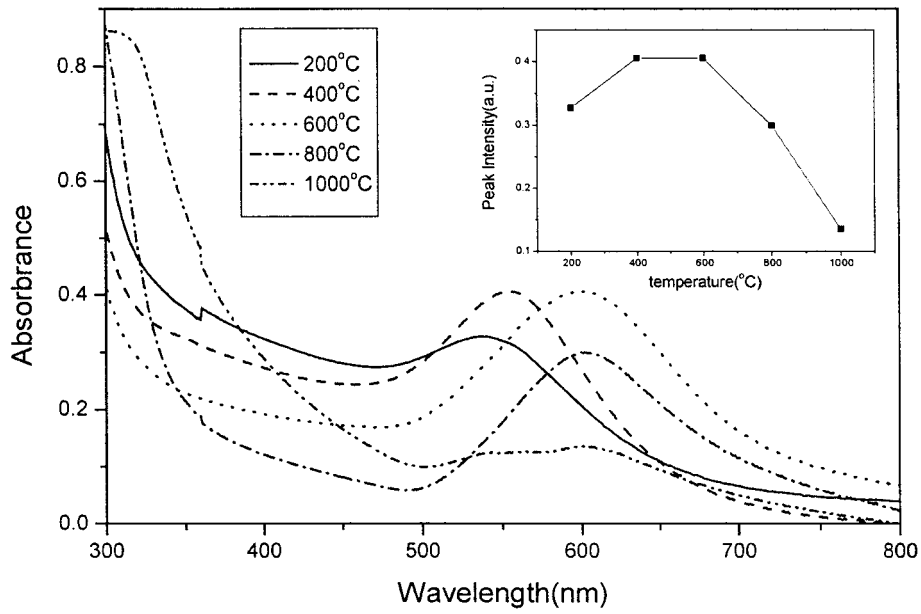

(b)

Figure 5 (a) Optical absorption spectra of Au/$BaTiO_3$ films annealed at different temperatures (coated on glass), the inset is the changes of absorption peak positions with annealing temperature and (b) Optical absorption spectra of Au/$BaTiO_3$ films annealed at different temperatures (coated on quartz glass), the inset is the changes of absorption intensities with annealing temperature.

with the increase of heat-treating temperature. The intensity of SPR peak increases with the increase of annealing temperature up to 600°C, and decreases with the continual increase of annealing temperature as showed in Fig. 5b. The intensity of SPR peak reaches the maximum at annealing temperature of 600°C.

The optical absorption coefficient of metal particles embedded in a dielectric matrix, determined through Mie theory [18], is described as follows:

$$\alpha = \frac{9q\omega}{c} n^3 \frac{\varepsilon_2(\omega; R)}{[\varepsilon_1(\omega; R) + (1/A - 1)n^2]^2 + \varepsilon_2(\omega; R)^2} \tag{1}$$

Where $\varepsilon(\omega; R) = \varepsilon_1(\omega; R) + i\varepsilon_2(\omega; R)$ is the dielectric function of metal particles; q is volume fraction of metal particle, and n is the refractive index of the surrounding matrix. The depolarization factor A is a function of particles' geometry and size. In the condition: $[\varepsilon_1(\omega; R) + (1/A - 1)n^2] = 0$, Mie resonance peak (Surface plasma resonance) will be attained. So the resonance peak is determined not only by the refractive index of surrounding matrix but also by the size of metal particles. Large particle size leads to a low value of A_{eff} and red-shifting of SPR peak. The increases of refractive index of matrix can also lead to red-shifting of SPR peak. In our experiment, metal particles sizes and refractive index of matrix both increase with annealing temperature. It is no doubt that Mie resonance peak will red-shift.

In the condition: $[\varepsilon_1(\omega; R) + (1/A - 1)n^2] = 0$, The intensity of SPR peak could be expressed by:

$$\alpha = \frac{9q\omega n^3}{c\varepsilon_{2(\omega,R)}} \tag{2}$$

In our experiment, with the increase of heat-treatment temperature, both the refractive index (n) of $BaTiO_3$ matrix and the radii of gold nanoparticles increase, which should lead to the increase of SPR intensity [19]. Such a change has been reported in Au/SiO_2 [20], Au/ZrO_2, [8] Au/TiO_2, [21] Ag/SiO_2-ZrO_2 [22] thin films and our samples heat-treated lower than 600°C. However, when Au/$BaTiO_3$ thin films were heat-treated at the temperature higher than 600°C, the SPR intensity decreases with the increase of heat-treatment temperature. This may be related to the self-polarization of $BaTiO_3$ ferroelectric matrix. When thin films were heat-treated at 600°C, $BaTiO_3$ perovskite crystallite formed and crystallized [23]. With the increase of heat-treating temperature, the perovskite structure grew more and more integrated, so the self-polarization effect turned stronger. This can generate an additional electric field E_{polar} outside of gold nanoparticles due to the self-polarization. The electric field E_{polar} can bind the oscillation of active surface electrons inside the gold particles, which should decrease the intensity of SPR peak [24].

3.5. Nonlinear optical properties

In this experiment, OKE was used to measure the values of third-order nonlinear susceptibility $\chi^{(3)}$ of Au/$BaTiO_3$ films. 800 nm pulse laser with a width of 120 fs was generated by Ti:Al_2O_3 femtosecond laser (Coherent Mira 900F), and 400 nm pulse was obtained by nonlinear frequency-doubled crystalline BBO (0.5 mm). 400 nm pulse was used as pump pulse and 800 nm pulse was used as probe beam. CS_2 was used as a standard sample, with its model of $\chi^{(3)}$ being 1.0×10^{-13} esu. The third-order nonlinear susceptibility $\chi^{(3)}$ (model) of thin film can be estimated with the following equation:

$$\chi^{(3)} = \left[\frac{I_s}{I_{ref}}\right]^{1/2}\left[\frac{n_s}{n_{ref}}\right]^2\left[\frac{L_{ref}}{L_s}\right]\frac{1}{R}\chi^{(3)}_{ref} \qquad (3)$$

Where n is the linear refractive index, I is the OKE signal intensity, L is the interaction distance of pump light and probe light in the sample, R is the correction coefficient, and suffices s and ref stand for sample and reference, respectively.

Fig. 6 shows the OKE signals of Au/$BaTiO_3$ films. The films exhibit ultra-fast nonlinear response, with their delay times of about 150 fs. The $\chi^{(3)}$ values of Au/$BaTiO_3$ films increase with increasing the heat-treatment temperature. The enhanced third-order nonlinear response of films should be attributed to the SPR peak position being closer to the laser pulse wavelength (800 nm) with the increase of heat-treatment temperature. The $\chi^{(3)}$ values of Au/$BaTiO_3$ films annealed at 500°C is $(3.8 \pm 0.8) \times 10^{-9}$ esu, which is two orders of magnitude larger than that of Au/ZrO_2 films [8] (It is difficult to compare the $\chi^{(3)}$ with reference [15] because the pulse wavelength and pulsewidth are unknown). The large values of $\chi^{(3)}$ in the Au/$BaTiO_3$ films should be attributed to high dielectric constant (or the refractive index) of the $BaTiO_3$ matrix and the high amount of Au particles incorporated in the matrix.

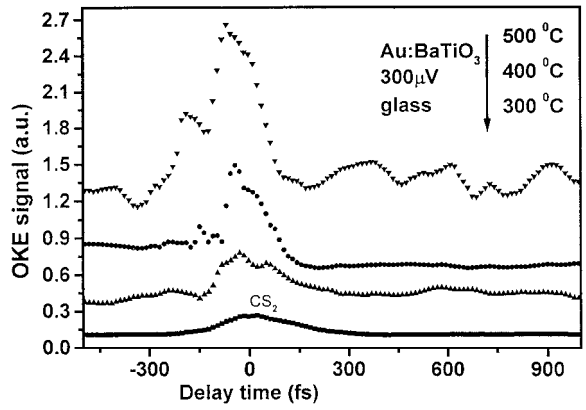

Figure 6 OKE signals of Au/$BaTiO_3$ films annealed at different annealing temperature.

According to Flytzanis [25], the third-order nonlinear susceptibility $\chi^{(3)}$ of metallic nanoparticles consists of three contributions: intraband contribution, interband contribution and hot electron contribution (nonequilibrium electron heating effect). The intraband contribution is strongly relative to the sizes of metal nanoparticles. Hache *et al.* [13] thought $\chi^{(3)}$ of metal particles was in inverse proportion to the diameter (R) of metal particles, $\chi^{(3)}$ should increases with the increase of the diameter of metal particles. However, this is not this case in our report. Based on the fact that there is no substantial size dependence of $\chi^{(3)}$, the dominant contribution should be that of the hot electron, but the interband contribution also plays an important role. The pump pulse energizes the conduction electrons, resulting in a high electronic temperature while the lattice remains cool. The electron heating leads to Fermi smearing, which affects the transition probability of the d-band electrons to the conduction band energies near the Fermi level, leading to changes in the reflectivity at the surface of the metal. The hot electron gas cools to the metal lattice through electron-phonon scattering [12]. The value of $\chi^{(3)}$ contributed by hot electrons is 10^{-6} esu. for gold particles [26]. Because the pump laser is far from the SPR peak position and the distribution of metal size is not narrow enough, the $\chi^{(3)}$ in our results is on the order of 10^{-9} esu. If the laser pulse wavelength is closer to the SPR peak position of metal particles, the third-order nonlinear susceptibilities will get enhanced largely.

4. Conclusions

Gold nanoparticles-dispersed $BaTiO_3$ films were prepared by the dip-coating method. Thiourea was applied to prevent Au ions from fast being reduced and aggregating as the effective capping and stabilization agents. A high amount of gold nanoparticles with an average size of 10 nm was incorporated in the $BaTiO_3$ matrix. The absorption spectra of Au/$BaTiO_3$ films exhibited a significant red shift of the SPR due to the changes of gold particles' size and refractive indices of those thin films. When Au/$BaTiO_3$ thin films were heat-treated at the temperature that was higher than 600°C, the SPR intensity decreases with the increase of heat-treatment temperature due to the influence of $BaTiO_3$ ferroelectric

matrix self-polarization. The nonlinear optical properties of these films was measured by a frequency-doubled Ti:Al_2O_3 femtosecond laser. The values of $\chi^{(3)}$ were calculated to be in the range of 10^{-8}–10^{-9} esu., which was two orders of magnitude higher than the reported value for Au/ZrO_2 films [7]. These films also exhibited superfast nonlinear response time and high third-order nonlinear susceptibilities, which would make these materials have more practical applications.

Acknowledgments

This research was supported by National Natural Science Foundation of China (Grant No. 50172057). The authors wish to thank Dr. Guohong Ma and Professor Shixiong Qian for the help in Nonlinear measurement and Professor Guangzhao Wu for the discussions.

References

1. WENJIANG NIE, *Adv. Mater*. **5** (1993) 520.
2. K. FUKUMI, A. CHAYAHARA, K. KADONO, Y. SAKAGUCHI, M. MIYA, K. FUJII, J. HAYAKAMA and M. SATOU, *J. Appl. Phys.* **75** (1994) 3075.
3. M. J. BLOEMER, J. W. HAUS and P. R. ASHLEY, *J. Opt. Soc. Am.* B **7** (1990) 790.
4. D. RICHARD, P. ROUSSIGNOL and C. FLYTZANIS, *Opt. Lett*. **10** (1985) 511.
5. S. A. KUCHINSKII and N. V. NIKONORO, *J. Non-Cryst. Solids*. **128** (1991) 109.
6. A. GOMBERT, W. GRAF, A. HEINZEL, R. JOERGER, M. KOHL and U. WEIMER, *Physica* A **207** (1994) 115.
7. D. F. EATON, *Science* **253** (1991) 281.
8. WEIMING HUANG and JIANLIN SHI, *J. Sol-Gel Sci. Tech.* **20** (2001) 145.
9. H. KOZUKA and S. SAKKA, *Chem. Mater*. **5** (1993) 222.
10. M. MENING, M. SCHMITT, U. BECHER, G. JUNG and H. SCHMITT, in SPIE: Sol-Gel Optics III, 1994, Vol. 2288, p. 130.
11. A. KAWABATA and R. KUBO, *J. Phys. Soc. Jpn.* **21** (1996) 1765.
12. R. REISFED, "Optical and Electronic Phenomena in Sol-Gel Glasses and Modern Application; Structure and Bonding 85" (Springer, Germany, 1996) p. 123.
13. F. HACHE, RICHARD and C. FLYTZANIS, *J. Opt. Soc. Am.* B **3** (1986) 1647.
14. JI ZHOU, LONGTU LI, ZHILUN GUI, XIAOWEN ZHANG and D. J. BARBER, *Nanostructured Materials* **3** (1997) 321.
15. SHIROU OTSUKI, KEISHI NISHIO, TOHRU KINERI, YUIICHI NATANADE and TOSHIO TSUCHIYA, *J. Am. Ceram. Soc.* **82** (1999) 1676.
16. M. EPIFANI, E. CARLINO, C. BLASI, C. GIANNINI, L. TAPFER and L. VASANELLI, *Chem. Mater*. **13** (2001) 1533.
17. REJI THOMAS, D. C. DUBE, M. N. KAMALASANAN and SUBHAS CHANDRA, *Thin Solid Films* **346** (1999) 212.
18. U. KREIBIG and M. VOLLMER, "Optical Properties of Metal Cluster" (Springer-Verlag, Berlin, 1995) p. 31.
19. P. B. JOHNSON and R. W. CHRISTY, *Phys. Rev*. B **6** (1972) 4370.
20. JUN MATSUOKA, RYOICHI MIZUTANI, SYOJI KANEKO *et al*., *J. Ceram. Soc. Jap.* **101** (1993) 53.
21. MINYUNG LEE, LEE CHAE and KYEONG CHUL LEE, *Nanostructured Materials* **11** (1999) 195.
22. F. GONELLA, G. MATTEI, P. MAZZOLDI *et al*., *Chem. Mater.* **11** (1999) 814.
23. MARIA C. GUST, NEAL D. EVANS, LESLIE A. MOMODA and MARTHAL L. MECARTNEY, *J. Am. Ceram. Soc.* **80** (1997) 2828.
24. U. KREIBIG and M. VOLLMER, "Optical Properties of Metal Cluster" (Springer-Verlag, Berlin, 1995) p. 24.
25. C. FLYTZANIS, in "Materials for Photonic Devices" (World Scientific, Singapore, 1991) p. 359.
26. S. SAKKA, H. KOZUKA and G. ZHAO, in SPIE: Sol-Gel Optics III, 1994, Vol. 2288, p. 108.

Received 20 March
and accepted 21 November 2002